

# A Way of Axion Detection with Mass $10^{-4}$ - $10^{-3}$ eV Using Cylindrical Sample with Low Electric Conductivity

Aiichi Iwazaki

*International Economics and Politics, Nishogakusha University,  
6-16 3-bantyo Chiyoda Tokyo 102-8336, Japan*

(Dated: Oct. 19, 2025)

A dark matter axion with mass  $m_a$  induces an oscillating electric field in a cylindrical sample placed under a magnetic field  $B$  parallel to the cylinder axis. When the cylinder is made of a highly electrically conductive material, the induced oscillating current flows only at the surface. In contrast, if the cylinder is composed of a material with small conductivity, e.g.  $\sigma = 10^{-3}$ eV, the electric current flows inside the bulk of the cylinder. Within the QCD axion model, the current  $I$  is estimated as  $I(m_a = 10^{-4}$ eV)  $\simeq 1.9 \times 10^{-14} A g_\gamma (R/6\text{cm})^2 (\sigma/10^{-3}\text{eV}) (B/10\text{T}) (10/\epsilon) (\rho_a/0.3\text{GeVcm}^{-3})$  with radius  $R$ , length  $L$ , permittivity  $\epsilon = 10$  of the cylinder and axion energy density  $\rho_a$ , where  $g_\gamma$  is model dependent parameter;  $g_\gamma(\text{KSVZ}) = -0.96$  and  $g_\gamma(\text{DFSZ}) = 0.37$ . Using an LC circuit with a quality factor  $Q = 10$ , the signal-to-noise ratio at temperature  $T = 100\text{mK}$  and observation time  $t_{ob} = 60\text{second}$  is  $\sim 0.5(Q/10) \sqrt{(m_a/10^{-4}\text{eV})(100\text{mK}/T)(t_{ob}/60\text{s})}$ . The detection of dark matter axions is feasible in the mass range  $m_a = 10^{-4}$ - $10^{-3}$ eV.

PACS numbers:

A central issue in particle physics is to identify phenomena beyond the Standard Model. The axion, proposed as the Nambu–Goldstone boson of Peccei–Quinn symmetry [1–3], provides a natural solution to the strong CP problem and is also a well-motivated dark matter candidate. It is called as QCD axion. The viable mass window for the QCD axion is tightly constrained to  $m_a = 10^{-6}$ - $10^{-3}$ eV [4–6].

Numerous experiments are underway to search for dark matter axions [7], most exploiting axion–photon conversion in a strong magnetic field. The induced electromagnetic radiation is expected to be detected with resonant cavities[8, 9], superconducting qubits[10], Quantum Hall effect [11, 12], e.t.c.

In this letter we propose a new method for axion detection using a cylindrical sample with small electrical conductivity,  $\sigma = 10^{-3}$ - $10^{-2}$ eV at low temperature 100mK. Our target is the mass range  $m_a = 10^{-4}$ - $10^{-3}$ eV, which is difficult to detect with resonant cavity.

Dark matter axion generates an oscillating electric field in the presence of a strong magnetic field, which in turn induces an oscillating current in the cylinder. By applying the magnetic field parallel to the cylinder axis, the induced current flows parallel to the external field.

In general, such currents are confined within the skin depth  $\delta$ . For highly conductive materials, e.g.  $\sigma = 10^4$ eV, the skin depth is extremely small ( $\delta \sim 10^{-5}\text{cm}$  for  $m_a = 10^{-4}\text{eV}$ ), restricting the current to a thin surface layer due to the induction effect. Additionally, electric field induced in the conducting material is suppressed by the factor  $\sqrt{m_a/\sigma} \sim 10^{-4}$ , compared with the one induced in vacuum. As a result, the electric current is not large enough to be detectable.

On the other hand, the two suppression factors do not arise for electromagnetic fields interacting with axion, Especially, for the cylinder sample with small conductivity, the induced current mainly flows the bulk, and the resulting electric current  $I$  becomes large enough to be detectable at low temperatures ( $T \sim 100\text{mK}$ ). We show that when the axion mass  $m_a = 10^{-4}$ eV,

$$I \simeq 2.1 \times 10^{-15} A g_\gamma \left( \frac{R}{2\text{cm}} \right)^2 \left( \frac{\sigma}{10^{-3}\text{eV}} \right) \left( \frac{B_0}{10\text{T}} \right) \left( \frac{10}{\epsilon} \right) \left( \frac{\rho_a}{0.3\text{GeVcm}^{-3}} \right) \quad (1)$$

with  $\sigma = 10m_a = 10^{-3}$ eV, where  $R$  denotes the radius of the cylinder with permittivity  $\epsilon = 10$ . The current is maximized by choosing electrical conductivity  $\sigma = \epsilon m_a$ , for instance,  $\sigma = 10^{-3}\text{eV}(m_a/10^{-4}\text{eV})$  when  $\epsilon = 10$ .  $I$  is proportional to the surface area  $R^2$ . The oscillating current flows the entire cylindrical sample, in contrast to ordinary electromagnetic induction where currents with high frequencies are confined to the surface.

In the actual measurement we compare the current  $I$  with current  $I_n$  of thermal noise. When the noise current  $I_n$  is smaller, the real signal current  $I$  can be observed more easily. Thus, it is favorable that the noise  $I_n$  is small. We adopt cylinder sample with small conductivity, e.g.  $\sigma = 10^{-3}$ eV, which causes large resistance  $R_c$  of the cylinder.

Because  $I_n \propto 1/\sqrt{R_c}$ , it is expected that the thermal noise  $I_n$  is small for large  $R_c$ . It is an advantage of using the sample with small conductivity  $\sigma = 10^{-3}\text{eV}$  for the axion detection. As we show later, we have

$$\frac{I}{I_n} \simeq 0.43 \times 10^{-4} g_\gamma \sqrt{\frac{100\text{mK}}{T}} \sqrt{\frac{\sigma}{10^{-3}\text{eV}}} \sqrt{\frac{10^{-4}\text{eV}}{m_a}} \sqrt{\frac{L}{100\text{cm}}} \left(\frac{R}{2\text{cm}}\right) \left(\frac{B_0}{10\text{T}}\right) \left(\frac{10}{\epsilon}\right) \left(\frac{\rho_a}{0.3\text{GeVcm}^{-3}}\right) \quad (2)$$

with length  $L$  of the cylinder.

By adopting an appropriate conductivity, e.g.  $\sigma \sim 5 \times 10^{-3}\text{eV}$  at low temperature  $\sim 20\text{mK}$  and radius ( length ) of the cylinder  $6\text{cm}$  (  $100\text{cm}$  ), we show that using parallel LC circuit tuned with a quality factor  $Q = 10$ , dark matter axion can be probed in the mass range  $m_a = 10^{-4}\text{-}10^{-3}\text{eV}$  with signal-noise ratio of the electric current bigger than 10.

Our method using cylinder with small electrical conductivity is also effective for so called, dark photon. The electromagnetic coupling with the dark photon gives rise to similar effect to the one in the QCD axion that oscillating electric current is induced in the whole of cylinder.

The main difficulty in detecting axion dark matter lies in its extremely weak coupling to electromagnetic radiation or ordinary matter ( electrons or nucleons ). In particular, the interaction between the axion field  $a(t, \vec{x})$  and the electromagnetic field is described by

$$L_{a\gamma\gamma} = g_{a\gamma\gamma} a(t, \vec{x}) \vec{E} \cdot \vec{B}, \quad (3)$$

where  $\vec{E}$  and  $\vec{B}$  denote the electric and magnetic fields, respectively. The coupling constant is  $g_{a\gamma\gamma} = g_\gamma \alpha / \pi f_a$ , with the fine structure constant  $\alpha \simeq 1/137$ , the axion decay constant  $f_a$ , and the relation  $m_a f_a \simeq 6 \times 10^{-6}\text{eV} \times 10^{12}\text{GeV}$  for the QCD axion model. The model dependent coefficient is  $g_\gamma \simeq 0.37$  for the DFSZ model [13, 14] and  $g_\gamma \simeq -0.96$  for the KSVZ model [15, 16].

For a classical axion field representing dark matter, the interaction term  $g_{a\gamma\gamma} a(t, \vec{x})$  is extremely small. Assuming that dark matter consists entirely of axions, the local energy density of the dark matter axion is

$$\rho_d = m_a^2 \overline{a(t, \vec{x})^2} = \frac{1}{2} m_a^2 a_0^2 \simeq 0.3\text{GeV}/\text{cm}^3, \quad (4)$$

where the overline denotes time averaging. This yields an effective CP-violating interaction of order  $g_{a\gamma\gamma} a(t, \vec{x}) \sim 10^{-21}$ , essentially independent of the QCD axion mass. Consequently, the axion-induced electric field in vacuum under an external magnetic field  $B_0$  is extremely weak, of order  $\sim g_{a\gamma\gamma} a B_0$ .

In this letter we show that, for a cylindrical sample in Fig.1 with small electrical conductivity, the electric current induced by axion dark matter can be large enough to be detectable at low temperatures  $T \sim 100\text{mK}$ . In this case, the current flows throughout the bulk of the cylinder, while for a good conductor with large conductivity, the current is confined to a thin surface layer.

We focus on the axion mass range  $m_a = 10^{-4}\text{-}10^{-3}\text{eV}$ , using a cylinder of length  $L = 100\text{cm}$ , radius  $R \geq 2\text{cm}$ , and conductivity  $\sigma = 10m_a = 10^{-3}\text{-}10^{-2}\text{eV}$ . As we show soon later, the condition of  $\sigma/m_a = \epsilon$  maximize the electric field induced in the cylinder with permittivity  $\epsilon$ . Such a matter with small conductivity may be realized at low temperatures  $\sim 100\text{mK}$ , for instance by using semiconductors with impurity doping appropriately.

A strong external magnetic field  $\vec{B}_0$  is applied parallel to the cylinder axis, so that the system is axially symmetric.  $\vec{B}_0 = (0, 0, B_0)$  in cylindrical coordinates  $(\rho, \theta, z)$ , with  $\rho = 0$  at the center and  $\rho = R$  at the surface of the cylinder. In the presence of dark matter axion, the magnetic field induces an oscillating current parallel to  $\vec{B}_0$ . This current produces microwave radiation with frequencies corresponding to axion masses in the range  $m_a = 10^{-4}\text{-}10^{-3}\text{eV}$ .

We calculate the axion-induced electric field  $E'$  to obtain oscillating electric current.

In order to obtain oscillating electric current  $\vec{J} = \sigma \vec{E}'$ , we solve the Maxwell equations involving axion effect,

$$\vec{\partial} \cdot (\epsilon \vec{E}' + g_{a\gamma\gamma} a(t, \vec{x}) \vec{B}) = 0, \quad \vec{\partial} \times (\vec{B} - g_{a\gamma\gamma} a(t, \vec{x}) \vec{E}') - \partial_t (\epsilon \vec{E}' + g_{a\gamma\gamma} a(t, \vec{x}) \vec{B}) = \vec{J}, \quad (5)$$

$$\vec{\partial} \cdot \vec{B} = 0, \quad \vec{\partial} \times \vec{E}' + \partial_t \vec{B} = 0 \quad (6)$$

where permittivity  $\epsilon$  and electric current  $\vec{J}$  are non vanishing inside the cylinder, while  $\epsilon = 1$  and  $\vec{J} = 0$  in vacuum. We have assumed trivial permeability  $\mu = 1$  of the cylinder.

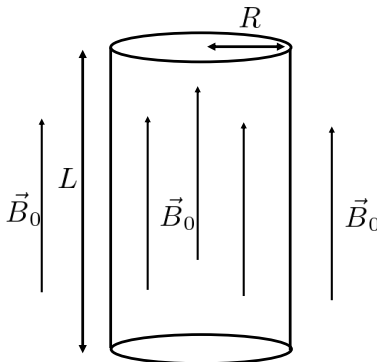


FIG. 1: cylinder sample with length  $L$  and radius  $R$  under external magnetic field  $\vec{B}_0$

The electric field  $\vec{E}'$  induced by the axion effect is much small, being of the order of  $g_{a\gamma\gamma}aB_0$ , while  $\vec{B} = \vec{B}_0 + \vec{B}'$  with external magnetic field  $\vec{B}_0 = (0, 0, B_0)$ .  $\vec{B}'$  is induced by the axion and associated with  $\vec{E}'$ .

It is easy to obtain the following equation of electric field  $\vec{E}'$  using cylindrical coordinate.

$$\left(\partial_\rho^2 + \frac{1}{\rho}\partial_\rho + \epsilon m_a^2 + i\sigma m_a\right)\vec{E}' = -m_a^2 g_{a\gamma\gamma} a(t) \vec{B}_0 \quad (7)$$

assuming  $a(t) \propto \exp(-im_a t)$ . The solution  $\vec{E}' = (0, 0, E')$  is

$$E' = d(t)J_0(bm_a\rho) + \frac{m_a^2 E_a}{\epsilon m_a^2 + im_a\sigma} \quad (8)$$

with  $E_a \equiv -g_{a\gamma\gamma}a(t)B_0$ , where  $d(t) \propto \exp(-im_a t)$  is a constant determined by boundary conditions at  $\rho = R$ . The corresponding magnetic field  $\vec{B}' = (0, B', 0)$  is given by solving  $\partial_t B' = \partial_\rho E'$ ,

$$B' = -ib d(t)J_1(bm_a\rho) \quad (9)$$

In the above expression,  $J_{0,1}(x)$  denotes Bessel function of the first kind and is chosen because of its finiteness of  $E'(\rho)$  at  $\rho = 0$ . The constant  $b$  is given by

$$b \equiv (\epsilon^2 + y^2)^{1/4} \exp(i\theta/2) \quad \text{with} \quad \theta = \cos^{-1}\left(\frac{\epsilon}{\sqrt{\epsilon^2 + y^2}}\right) \quad (10)$$

with  $y \equiv \sigma/m_a$ .

These solutions  $E'$  and  $B'$  represent electric and magnetic fields inside the cylinder with radius  $R$ . Similarly, we can find solutions  $E_v$  and  $B_v$  outside the cylinder with the conditions  $\vec{J} = 0$  and  $\epsilon = 1$  in the Maxwell equations.

$$E_v = \tilde{d}(t)H_0^{(1)}(m_a\rho) + E_a \quad \text{and} \quad B_v = -i\tilde{d}(t)H_1^{(1)}(m_a\rho) \quad (11)$$

with  $H_{0,1}^{(1)}$  Hankel functions of the first kind, where  $\tilde{d} \propto \exp(-im_a t)$  is a constant determined by boundary conditions at  $\rho = R$ . The Hankel function of the first kind is chosen because the radiations described by  $E_v$  and  $B_v$  are outgoing waves;  $E_v(B_v) \sim \exp(-im_a t + im_a\rho)$  as  $\rho \rightarrow \infty$ .

In order to determine the constants  $d(t)$  and  $\tilde{d}(t)$ , we impose boundary conditions at the surface  $\rho = R$  of the cylinder such that  $\epsilon E'(\rho = R) = E_v(\rho = R)$  and  $B'(\rho = R) = B_v(\rho = R)$ . Then, we have

$$\epsilon d(t)J_0(bm_a R) + \frac{\epsilon m_a^2 E_a}{\epsilon m_a^2 + i m_a \sigma} = \tilde{d}(t)H_0^{(1)}(m_a R) + E_a \quad \text{and} \quad b d(t)J_1(bm_a R) = \tilde{d}(t)H_1^{(1)}(m_a R) \quad (12)$$

Therefore, by solving the equations for  $d(t)$  and  $\tilde{d}(t)$ , we have

$$d(t) = \frac{iy}{\epsilon + iy} \frac{E_a H_1^{(1)}(x)}{\epsilon J_0(bx)H_1^{(1)}(x) - bJ_1(bx)H_0^{(1)}(x)}, \quad \tilde{d}(t) = d(t) \left( \frac{bJ_1(bx)}{H_1^{(1)}(x)} \right), \quad (13)$$

with  $x = m_a R$ .

Thus, the oscillating electric and magnetic fields  $E'$  and  $B'$  inside the cylinder are

$$E'(\rho) = E_a \left( \frac{1}{\epsilon + iy} + \frac{iy}{\epsilon + iy} \frac{H_1^{(1)}(m_a R)J_0(bm_a \rho)}{\epsilon J_0(bm_a R)H_1^{(1)}(m_a R) - bJ_1(bm_a R)H_0^{(1)}(m_a R)} \right) \quad (14)$$

$$B'(\rho) = E_a \left( \frac{by}{\epsilon + iy} \frac{E_a H_1^{(1)}(m_a R)J_1(bm_a \rho)}{\epsilon J_0(bm_a R)H_1^{(1)}(m_a R) - bJ_1(bm_a R)H_0^{(1)}(m_a R)} \right). \quad (15)$$

They oscillate as  $E'(B') \propto \exp(-im_a t)$ . Obviously, the first term of the electric field,  $E'(\rho)$ , exists throughout the bulk of the cylinder, whereas the second term is confined to its surface;  $J_0(bm_a \rho)/J_{0,1}(bm_a R) \propto \exp((R-\rho)m_a \text{Im}(b))$  as  $\rho \rightarrow \infty$  where  $\text{Im}(O)$  denotes imaginary part of  $O$ .

Uniquely, the axion–electromagnetic coupling drives an oscillating electric field that permeates the entire cylindrical sample, in contrast to ordinary electromagnetic induction, where the high frequency electric field is confined to the surface. A similar fact is also present in the case of dark photon[17].

As shown later, the second term dominates the electric power ( Joule heat ) in the limit of large conductivity ( $\sigma \sim 10^4 \text{eV}$ ), while the first term becomes dominant for small conductivity ( $\sigma \sim 10^{-3} \text{eV}$ ).

Using the formula of the electric field  $E'$ , we obtain oscillating electric current  $J(\rho) = \sigma R e(E'(\rho))$  and corresponding its power  $P$  averaged over the period  $2\pi/m_a$ ,

$$P = \int_0^R \overline{J(\rho)(Re(E'(\rho)))} L 2\pi \rho d\rho = \int_0^R \sigma |E'(\rho)|^2 L \pi \rho d\rho \quad (16)$$

where  $Re(O)$  denotes real part of the quantity  $O$ .

When we put  $z = \rho/R$ , the formula  $P$  is rewritten such that

$$P = \sigma L \pi \int_0^1 |E'(Rz)|^2 R^2 z dz = \frac{\pi L |E_a|^2}{m_a} \int_0^1 y x^2 |U(x, y, z)|^2 z dz, \quad (17)$$

where  $U(x, y, z)$  is

$$U(x, y, z) \equiv \frac{1}{\epsilon + iy} + \frac{iy}{\epsilon + iy} \frac{H_1^{(1)}(x)J_0(bxz)}{\epsilon J_0(bx)H_1^{(1)}(x) - bJ_1(bx)H_0^{(1)}(x)} \quad (18)$$

We remind that  $y \equiv \sigma/m_a$  and  $x \equiv m_a R$  and  $b = b(y)$  is the function of  $y$ .  $P$  is a complicated function in  $x$  and  $y$ , or  $m_a$  and  $R$ . But we show below that  $P$  becomes a simple function in  $x$  and  $y$  when we take the limit of large conductivity,  $\sigma \sim 10^4 \text{eV}$  or small  $\sigma \sim 10^{-3} \text{eV}$ . We note that electric field is written such that  $E'(\rho) = E_a U$ .

It is easy to confirm that in the limit of  $\sigma \rightarrow \infty$  ( $y \rightarrow \infty$ ),  $P \propto m_a \rho_a V (B_0/m_a M)^2 |H_1^{(1)}(x)/H_0^{(1)}(x)|^2$  with  $M \equiv \pi f_a/(g_\gamma \alpha)$  and the volume  $V = 2\pi R L \delta$ , within which the electric current flows.  $\delta = \sqrt{2/m_a \sigma}$  denotes skin depth. The current flows only in the surface with the depth  $\delta$  of the cylinder. It is coincide with the previous result [17]. In the limit, the main contribution comes from the second term in  $U$ . We note that  $|H_1^{(1)}(x)/H_0^{(1)}(x)|^2 \simeq 1$  for  $x > 5$ .

The skin depth for general  $\sigma$  represented by the second term of  $U(x, y, z)$  in eq(18) is given by  $(m_a \text{Im}(b(y)))^{-1} = (m_a(\epsilon^2 + (\sigma/m_a)^2)^{1/4} \sin(\theta/2))^{-1} > \delta = \sqrt{2/m_a\sigma}$ . In this paper, assuming typical value  $\epsilon = 10$  in semiconductor, we take small electric conductivity  $\sigma \sim \epsilon m_a \sim 10m_a$  ( $y \sim 10$ ) and consider the mass region  $m_a = 10^{-3}-10^{-4}\text{eV}$ . Then, the skin depth  $(m_a \text{Im}(b(y)))^{-1} \simeq 0.1\text{cm}(10^{-4}\text{eV}/m_a)$ , smaller than the radius  $R = 2\text{cm}$  examined in our paper. On the other hand, the first term of  $U$  is present in the whole of the cylinder, not confined at the surface.

In such a cylinder with small electrical conductivity, we find that the main contribution to  $P$  comes from the first term in  $U$ . Actually, the following quantities are monotonically increasing function in  $x$ ,

$$\int_0^1 yx^2 dz \left| \frac{iy}{\epsilon + iy} \frac{H_1^{(1)}(x)J_0(bxz)}{\epsilon J_0(bx)H_1^{(1)}(x) - bJ_1(bx)H_0^{(1)}(x)} \right|^2 = 0.01-0.09 \text{ for } x = 1-10 \quad (19)$$

$$\int_0^1 yx^2 dz \left| \frac{1}{\epsilon + iy} \right|^2 = 0.025-2.5 \text{ for } x = 1-10. \quad (20)$$

with  $y = 10$  and  $\epsilon = 10$ . We find that for each  $x$ , the quantity in the second equation is larger than the one in the first equation. Especially, it is more than an order of magnitude for  $x \geq 10$ . Further, smaller  $y$  ( $< 10$ ) leads to much larger discrepancy between the quantities. Therefore, we may write

$$P = \frac{\pi L |E_a|^2}{m_a} \int_0^1 yx^2 |U(x, y, z)|^2 dz \sim \frac{\pi L |E_a|^2}{2m_a} \left( \frac{yx^2}{\epsilon^2 + y^2} \right). \quad (21)$$

$P$  takes the maximal value at  $y = \sigma/m_a = \epsilon$  and  $P(\epsilon, y = \epsilon) \propto \epsilon^{-1}$ . Thus, it is favorable to take the conductivity  $\sigma = \epsilon m_a$ . Because we do not know the value of the axion mass  $m_a$ , the value  $\sigma = \epsilon m_a$  is unknown. But when we put  $\sigma = \epsilon m_a$  in the formula, the dependence of  $P$  on  $m_a$  becomes simple;  $P \propto m_a$ . In the actual search of the axion mass in the range  $10^{-4}-10^{-3}\text{eV}$ , it is sufficient for the axion detection to take the value  $\sigma \sim 5 \times 10^{-3}\text{eV}$  with  $\epsilon \sim 10$ . Although it does not lead to the maximal power  $P$ , the predicted signal-noise ratios are large enough for the detection. Hereafter we take  $\sigma = \epsilon m_a$  and  $\epsilon = 10$  for simplicity.

Numerically, noting  $|E_a| = |g_{a\gamma\gamma} a(t) B_0| \simeq 1.6 \times 10^{-36} \text{GeV}^2 g_\gamma(B_0/10\text{T})$ , we find

$$P(\sigma = 10^{-3}\text{eV}) \simeq 2.8 \times 10^{-28} \text{W} g_\gamma^2 \left( \frac{L}{100\text{cm}} \right) \left( \frac{R}{2\text{cm}} \right)^2 \left( \frac{B_0}{10\text{T}} \right)^2 \left( \frac{m_a}{10^{-4}\text{eV}} \right) \left( \frac{10}{\epsilon} \right) \left( \frac{\rho_a}{0.3\text{GeVcm}^{-3}} \right) \quad (22)$$

with  $\epsilon = 10$ ,  $y = 10$  ( $\sigma = 10m_a$ ) and  $x \simeq 10$  ( $R = 2\text{cm}$ ). Obviously,  $P$  in eq.(21) is proportional to  $R^2 = x^2/m_a^2$ , that is, the cross section  $\pi R^2$  of the cylinder. The energy dissipation takes place in the bulk volume  $\propto R^2 L$ , not merely in the surface, resulting in substantially enhanced dissipation power  $P$ .

For comparison, we present the power  $P$  when the conductivity is much high,  $\sigma = 10^4\text{eV}$ ,

$$P(\sigma = 10^4\text{eV}) \simeq |E_a|^2 \frac{\pi m_a \delta R L}{2} \left| \frac{H_1^{(1)}(x)}{H_0^{(1)}(x)} \right|^2 \quad (23)$$

$$\simeq 8.0 \times 10^{-32} \text{W} g_\gamma^2 \left( \frac{L}{100\text{cm}} \right) \left( \frac{R}{2\text{cm}} \right) \sqrt{\frac{m_a}{10^{-4}\text{eV}}} \sqrt{\frac{10^4\text{eV}}{\sigma}} \left( \frac{B_0}{10\text{T}} \right)^2 \left( \frac{\rho_a}{0.3\text{GeVcm}^{-3}} \right) \quad (24)$$

with  $y = \sigma/m_a = 10^8$  and  $x = m_a R \simeq 10$ . It is generated in the surface with the skin depth  $\delta \sim 10^{-5}\text{cm}$  of the cylinder. We find that the power  $P(\sigma = 10^{-3}\text{eV})$  with small conductivity, is three order of magnitude larger than  $P(\sigma = 10^4\text{eV})$  with large conductivity. That is,  $P(\sigma = 10^{-3}\text{eV}) > 10^3 P(\sigma = 10^4\text{eV})$ . It is the reason why we use such a cylinder with small conductivity  $\sigma \sim 10^{-3}\text{eV}$ .

There are two reasons of the small power  $P(\sigma = 10^4\text{eV})$  in the cylinder. One is the suppression of electric field inside conductor with large conductivity  $\sigma = 10^4\text{eV}$ , that is,  $\sqrt{m_a/\sigma} |E_a|$  [12, 17] compared with  $|E_a|/2\epsilon$  in material with small conductivity  $\sigma = 10^{-3}\text{eV}$ . The other one is the presence of the skin depth  $\delta = \sqrt{2/m_a\sigma}$ . The area  $2\pi R\delta$  of the current flowing is much smaller than that  $\pi R^2$  in material with low conductivity. Therefore, even if large conductivity  $\sigma$  amplifies electric current by the factor  $\sigma$ , both the suppression of electric field by the factor  $\sqrt{m_a/\sigma}$  and the area of current flow by the factor  $\sqrt{1/m_a\sigma}$ , cause the power  $P(\sigma = 10^4\text{eV})$  smaller than the power  $P(\sigma = 10^{-3}\text{eV})$ . It is roughly,

$$\frac{P(\sigma_h = 10^4 \text{eV})}{P(\sigma = 10^{-3} \text{eV})} \sim \frac{R\delta\sigma_h(\sqrt{m_a/\sigma_h})^2}{R^2\sigma(1/\epsilon^2)} = \frac{\delta m_a \epsilon^2}{R\sigma} \sim 10^{-3} \quad (25)$$

with  $R = 1\text{cm}$ ,  $\epsilon = 10$  and  $m_a = 10^{-4}\text{eV}$ . It is coincident with the above calculations in eq(22) and eq(23).

The large power  $P(\sigma = 10^{-3}\text{eV})$  arises mainly from large electric current  $I$  flowing in the bulk of the cylinder. The electric current  $I$  is,

$$I(\sigma = 10^{-3}\text{eV}) = \frac{\sigma|E_a|S}{2\epsilon} \simeq 2.1 \times 10^{-15} \text{A} g_\gamma \left(\frac{R}{2\text{cm}}\right)^2 \left(\frac{\sigma}{10^{-3}\text{eV}}\right) \left(\frac{B_0}{10\text{T}}\right), \quad (26)$$

where the electric field  $E = \text{Re}(E') = |E_a|/2\epsilon = |E_a|/20$  is the one in the first term with  $y = 10$  in eq(14). We detect the axion by measuring the large electric current  $I$ .

The point causing the large current  $I$  is that electric field  $E$  inside of the cylinder with small conductivity, e.g.  $\sigma = 10^{-3}\text{eV}$  has no suppression factor  $\sqrt{m_a/\sigma} \simeq 10^{-4}$ , which is present when the cylinder with large conductivity  $\sigma = 10^4\text{eV}$ . Additionally, the current flows in the whole of the cylinder, not just in the surface. The facts make the large electric current  $I$  to be observable.

There is another point which makes axion detection feasible. In the actual observation, we need to take into account thermal noise ( Johnson-Nyquist noise ). The electric current  $I_n$  by the thermal noise is given by  $I_n = \sqrt{2T\delta\omega/\pi R_c}$  with temperature  $T = 100\text{mK}$  and the width  $\delta\omega$  of the frequency;  $\delta\omega = 10^{-6}m_a = 10^{-10}(m_a/10^{-4}\text{eV})\text{eV}$ .  $R_c = L/(\sigma S)$  with  $S = \pi R^2$  denotes electric resistance of the cylinder;  $R_c = 0.16(L/100\text{cm})(2\text{cm}/R)^2$ . Then we find

$$I_n = 4.9 \times 10^{-11} \text{A} \sqrt{\left(\frac{T}{100\text{mK}}\right) \left(\frac{m_a}{10^{-4}\text{eV}}\right) \left(\frac{\sigma}{10^{-3}\text{eV}}\right) \left(\frac{100\text{cm}}{L}\right) \left(\frac{R}{2\text{cm}}\right)^2}. \quad (27)$$

Because the noise  $I_n \propto 1/\sqrt{R_c}$ , the noise is small for the large resistance  $R_c \simeq 0.16$  of the cylinder. It should be stressed that the small noise  $I_n$  is caused by small electrical conductivity  $\sigma = 10^{-3}\text{eV}$  of the cylinder. Thus, we obtain the ratio of the current  $I$  to the noise  $I_n$ ,

$$\frac{I(\sigma = 10^{-3}\text{eV})}{I_n(\sigma = 10^{-3}\text{eV})} \simeq 0.43 \times 10^{-4} g_\gamma \sqrt{\frac{100\text{mK}}{T}} \sqrt{\frac{\sigma}{10^{-3}\text{eV}}} \sqrt{\frac{10^{-4}\text{eV}}{m_a}} \sqrt{\frac{L}{100\text{cm}}} \left(\frac{R}{2\text{cm}}\right) \left(\frac{B_0}{10\text{T}}\right) \left(\frac{\rho_a}{0.3\text{GeVcm}^{-3}}\right) \quad (28)$$

In order to amplify the above ratio  $I/I_n$ , we use, for instance, parallel LC circuit with resistance  $R_c$ , inductance  $L_c$  and capacitance  $C_c$ . ( The resistance  $R_c$  in the parallel LC circuit is almost equal to the one of the cylinder. ) When we tune the circuit with resonant frequency  $\omega = \sqrt{1/L_c C_c} = m_a$  and a quality factor  $Q$  such as  $Q = R_c \sqrt{C_c/L_c}$ , the above ratio is amplified such as  $Q(I/I_n)$ . In actual experiment, it is difficult to have large quality factor  $Q$  such as  $Q > 10^3$ . So we assume  $Q = 10$  as a realistic value and measure the electric current in the coil of the LC circuit. Furthermore, in the measurement of the oscillating current, we take the frequency width  $\delta\omega = 10^{-6}m_a$  and observation time 60 seconds. Then, the actual noise is reduced as  $I_n/\sqrt{\delta\omega\delta t_{ob}/(2\pi)} \simeq I_n/(1.2 \times 10^3 \sqrt{\frac{m_a}{10^{-4}\text{eV}} \sqrt{\frac{t_{ob}}{60\text{s}}}})$ .

It follows that the signal-noise ( SN ) ratio is

$$\frac{I(\sigma = 10^{-3}\text{eV})}{I_n(\sigma = 10^{-3}\text{eV})} Q \sqrt{\frac{\delta\omega t_{ob}}{2\pi}} \simeq 0.51 g_\gamma \left(\frac{Q}{10}\right) \sqrt{\frac{100\text{mK}}{T}} \sqrt{\frac{t_{ob}}{60\text{s}}} \sqrt{\frac{\sigma}{10^{-3}\text{eV}}} \sqrt{\frac{L}{100\text{cm}}} \left(\frac{R}{2\text{cm}}\right) \left(\frac{B_0}{10\text{T}}\right) \left(\frac{\rho_a}{0.3\text{GeVcm}^{-3}}\right) \quad (29)$$

with  $y = 10$  and  $x \simeq 10$ , where  $t_{ob} = 60$  s denotes the observation time. Although the SN ratio does not explicitly involve the axion mass  $m_a$ , it implicitly depends on  $m_a$  because  $\sigma$  is taken as  $\sigma = 10m_a$ . When we searches  $m_a = 10^{-3}\text{eV}$ , it is favorable to have  $\sigma = 10^{-2}\text{eV}$ . Then, the SN ratio is  $\simeq 1.6$ .

Therefore, it turns out that by the observation of the electric current  $I$  with appropriate choices of, for instance, temperature  $T = 20\text{mK}$  and the radius  $R = 6\text{cm}$ , and observation time  $t_{ob} = 600$  s, SN ratio is larger than 10. Without such a choice of the parameters, we can obtain large SN ratio as far as we tune quality factor  $Q$  bigger than 10.

We point out that when we search much larger axion mass  $m_a > 10^{-3}\text{eV}$ , it is easier to detect such axions This is because electric current  $I \propto \sigma$  and SN ratio  $\propto \sqrt{\sigma}$  are much larger than those of  $m_a = 10^{-3}\text{eV}$  with the appropriate choice of conductivity  $\sigma = 10m_a$ .

We find that the method of the axion detection using cylinder sample with small electrical conductivity is very powerful. This is because the axion–electromagnetic coupling induces an oscillating electric field  $|E_a|/2\epsilon$  throughout the entire cylindrical sample, producing sufficiently large electric current  $I \propto \sigma(|E_a|/\epsilon)^2 R^2$  for the detection. Furthermore, the sample with small electrical conductivity has small thermal noise compared with the one with large electrical conductivity.

Summarized, we have proposed a method for axion detection with a cylindrical sample choosing appropriate small conductivity ( $\sigma = 10^{-3}$ - $10^{-2}$ eV) sensitive to microwave signals in the frequency range  $m_a/2\pi = 24$ - $240$ GHz. With such conductivity, the axion induces large electric current flowing the bulk of the cylinder and causes a high signal-to-noise ratio of the current. Therefore, the method demonstrates the feasibility of detecting dark matter axions under realistic experimental conditions. It is also effective for the search of dark photon.

- 
- [1] R. D. Peccei and H. R. Quinn, Phys. Rev. Lett. 38 (1977) 1440.
  - [2] S. Weinberg, Phys. Rev. Lett. 40 (1978) 223.
  - [3] F. Wilczek, Phys. Rev. Lett. 40 (1978) 279.
  - [4] J. Preskill, M. B. Wise and F. Wilczek, Phys. Lett. 120B (1983) 127.
  - [5] L. F. Abbott and P. Sikivie, Phys. Lett. B120 (1983) 133.
  - [6] M. Dine and W. Fischler, Phys. Lett. B120 (1983) 137.
  - [7] Maurizio Giannotti, arXiv: 2412.08733.
  - [8] C. Goodman, et al, Phys. Rev. Lett. 134, (2025) 111002.
  - [9] Xiran. Bai, et al. Phys. Rev. Lett. 134 (2025) 15.
  - [10] Phys. Rev. Lett. 131 (2023) 21, 211001.
  - [11] A. Iwazaki, arXiv: 2508.01123.
  - [12] A. Iwazaki, PTEP 2024 (2024) 6, 063C01.
  - [13] M. Dine, W. Fischler and M. Srednicki, Phys. Lett. 104B (1981) 199.
  - [14] A. R. Zhitnitsky, Sov. J. Nucl. Phys. 31 (1980) 260.
  - [15] J. E. Kim, Phys. Rev. Lett. 43, (1979) 103.
  - [16] M. A. Shifman, A. I. Vainshtein and V. I. Zakharov, Nucl. Phys. B166 (1980) 493.
  - [17] Y. Kishimoto and K. Nakayama, Phys. Lett. B 827 (2022) 136950.